International Journal of Research and Review
[Indexed, Peer-Reviewed Journal]
Volume 12; Issue: 9; September 2025
Website: www.ijrrjournal.com
Research Paper *E-ISSN: 2349-9788; P-ISSN: 2454-2237*

Adaptive Tracking Control for Dynamic Model Uncertainties of a 6-DOF Industrial Staubli Robot Manipulator Carrying Variable Payloads

Emir Sonmez[1], Kamil Cetin[1,2]

[1]Department of Electrical & Electronics Engineering, Izmir Katip Celebi University, Izmir, 35620 Turkiye,
[2]Smart Factory Systems Application & Research Center, Izmir Katip Celebi University, Izmir, 35620 Turkiye.

Corresponding Author: Kamil Cetin

DOI: https://doi.org/10.52403/ijrr.20250963

ABSTRACT

This work introduces the design of an adaptive tracking control strategy for a 6-DOF Staubli TX2-60L industrial robot manipulator operating under dynamic model uncertainties caused by variable payloads. A complete kinematic and dynamic model of the robot is derived using Denavit–Hartenberg parameters and the Lagrangian formulation, respectively. To address the limitations of conventional control methods under payload variations, an adaptive controller is designed, which continuously updates its parameters based on real-time tracking errors. A Lyapunov stability analysis is conducted to rigorously establish that the closed-loop system guarantees convergent tracking errors and bounded internal states. Simulation studies with different payload scenarios, including no load, step load variation, and continuous load changes, show the performance of the proposed control strategy. The results confirm that the adaptive controller maintains precise trajectory tracking and robust stability despite significant model uncertainties, highlighting its suitability for industrial pick-and-place and high-precision automation tasks.

Keywords: Robot manipulator, kinematic model, dynamic model, variable payloads, adaptive control, stability analysis.

INTRODUCTION

Industrial robot arms are widely used in numerous applications due to their superior speed, precision, and reliability [1]. Their robust mechanical design, ease of maintenance and the ability to operate continuously without significant errors make them highly suitable for hazardous tasks that pose risks to human life, as well as for automation processes aimed at reducing human workload [2, 3]. The integration of advanced motor and sensor technologies further enables these systems to achieve the high levels of accuracy required in delicate operations such as welding, laser cutting, and pick-and-place tasks [3]. To perform such precision-demanding tasks, robot arms must be equipped not only with sophisticated actuation and sensing capabilities but also with powerful control architectures. Robots that combine these features have become indispensable assets in modern industry.

This study addresses the design of a robust controller for industrial robot arms that perform tasks where both accuracy and safety are paramount. One of the main challenges in controlling such systems is maintaining stability and precision in the presence of uncertainties or variations of the dynamic model of the robot arm [4]. Although the conventional PID controller remains one of the most widely applied methods, it has notable limitations: its simplicity makes it prone to performance

degradation and even instability under fast or high-acceleration movements in uncertain or disturbed environments [5]. To overcome these limitations, recent research has increasingly focused on advanced adaptive control strategies, which provide greater resilience and reliability in dynamic industrial settings.

A wide range of adaptive control strategies have been explored in the literature to address uncertainties in robotic arm dynamics. Traditional manipulator control systems often fall short of meeting the increasing demands of modern industrial applications, motivating the adoption of adaptive neural network–based methods that improve trajectory tracking under system uncertainties and external disturbances [6]. Similarly, Adaptive Degrees-of-Freedom (DoF) Mapping Control, particularly when integrated with feed-forward multimodal feedback, has been shown to reduce task completion time, minimize mode switches, and lower perceived workload [7]. In the aerospace domain, fuzzy-compensated sliding mode control has been demonstrated to reduce trajectory tracking errors in flexible space manipulators, outperforming classical sliding mode control methods under nonlinear uncertainties and disturbance torques [8]. For collaborative settings, two-loop adaptive control structures that combine sliding mode control for load-side uncertainties with model reference adaptive control for motor-side dynamics have also yielded notable performance improvements [9]. In soft robotics, reinforcement learning–driven adaptive control schemes have emerged to address stochastic behavior and the training-to-reality gap, enabling precise task execution and resilience even under actuation damage [10]. Likewise, adaptive neural network controllers based on radial basis function (RBF) models and Lyapunov stability analysis have been applied to multi-DoF manipulators in logistics and agriculture, ensuring stable and robust motion control [11]. Other work has introduced Fourier series–based adaptive observer–controllers to guarantee stable pose and force regulation in systems with unmodeled dynamics and unmeasurable joint velocities [12]. Extending robotic arms onto mobile platforms has also been studied, where model reference adaptive control strategies improve trajectory tracking robustness against model uncertainties [13]. In heavy industrial contexts, fractional-order model reference adaptive control (FOMRAC) has been proposed as a more resilient alternative to conventional MRAC, showing superior results in positioning accuracy and disturbance rejection [14]. Adaptive backstepping control has likewise been applied to flexible joint arms, with Lagrange–Euler modeling confirming robust tracking without overshoot, even under parameter variations and input saturation [15]. Fault tolerance has been addressed through robust hybrid predictive control (HFTPC), where actuator faults and time delays in hybrid electric–pneumatic systems are mitigated using linear matrix inequality–based stability conditions [16]. Cooperative manipulation has also been advanced through distributed controllers with online payload estimation and wrench-synthetic trajectory tracking, ensuring bounded tracking errors despite uncertain grasp positions and external disturbances [17]. Further contributions include the development of robust adaptive fuzzy sliding mode controllers, which combine fuzzy logic approximation with adaptive parameter laws to improve accuracy and disturbance rejection in serial manipulators [18]. Path planning innovations, such as improved RRT-Connect algorithms with adaptive step strategies and multi-tree sampling, have enhanced efficiency in application-specific tasks like exhaust emission detection [19]. Finally, in compliant industrial interactions, adaptive control frameworks integrating dynamic movement primitives (DMPs), impedance control, and admittance adaptation have demonstrated stable force regulation and improved conformity in precision tasks such as surface grinding [20]. As can be seen from the above studies, there has not been much research in the literature

on the adaptive control of industrial robot arms. Although there are studies on adaptive control of robot arms, particularly in response to uncertainties in dynamic models, the precise control of robot arms in industrial applications, particularly in response to variations in their payloads, has not been adequately studied. This study focuses on adaptive control of industrial robot arms, particularly in response to changes in their payloads. In this paper, we present the development and validation of an adaptive tracking control strategy for a 6-DOF Staubli TX2-60L industrial robot manipulator subjected to dynamic model uncertainties caused by variable payloads. First, the complete kinematic and dynamic models of the manipulator are derived using the Denavit–Hartenberg method and the Lagrangian formulation, respectively, providing the mathematical basis for control design. Building upon this, an adaptive controller is designed with online parameter adjustment to address the limitations of conventional control methods under changing load conditions. The stability of the proposed control method is rigorously verified through Lyapunov-based analysis, ensuring convergence of position and velocity tracking errors. Finally, extensive simulation studies under different payload scenarios, including no load, step load variations, and continuous load changes, are conducted to demonstrate the robustness and effectiveness of the controller in maintaining precise trajectory tracking and stable system responses.

KINEMATIC MODEL OF STAUBLI ROBOT ARM

Forward Kinematics Model

Kinematics is the branch of mechanics that is concerned with describing the motion of bodies without reference to the forces that cause this motion. This process requires computation of the time derivatives, including velocity, acceleration, and higher-order terms of the robot's position variables. In robotics, the kinematic model provides a mathematical framework to describe geometric relationships and movement between the joints of a manipulator. This modeling is essential for calculating the necessary joint motions to track a desired trajectory. The Denavit-Hartenberg (DH) parameters define the relative robot joints' transformation matrices, forming a systematic foundation for representing kinematic chains. An industrial Staubli TX2-60L robot manipulator is illustrated in Fig. 1.

Fig. 1: Staubli TX2-60L industrial robot manipulator.

Fig. 2 shows the assigned frames of the Staubli robot manipulator.

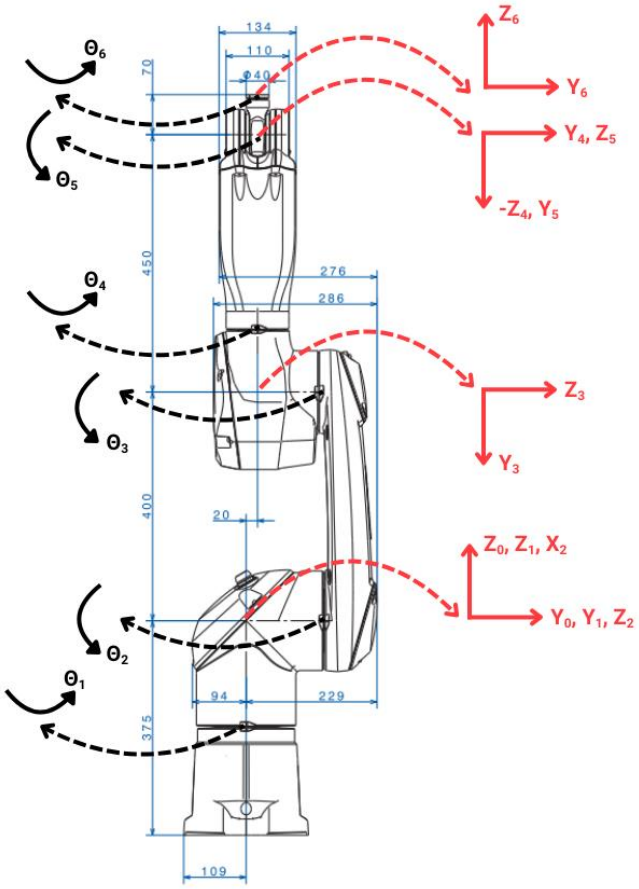

Fig. 2: Schematic of the Staubli Robot Manipulator with frame assignments.

Table I presents the DH parameters of the Staubli robot manipulator.

TABLE I: Denavit-Hartenberg (DH) Parameters.

i	α	a_{i-1} (m)	d_{i-1} (m)	θ
1	0	0	0	θ_1
2	$-\pi/2$	0	0	θ_2
3	0	a_2	d_3	θ_3
4	$\pi/2$	0	d_4	θ_4
5	$-\pi/2$	0	0	θ_5
6	$\pi/2$	0	$d_6 0$	θ_6

The link frames and their corresponding parameters are defined in Fig. 2 and Table I. Once the link frames and associated link parameters are specified, formulating the kinematic equations becomes straightforward. With the values of the link parameters, the individual link transformation matrices can be calculated. These matrices are then multiplied sequentially to obtain the overall transformation matrix that relates frame {N} to the base frame {0}.

$$ {}^{0}_{N}T = {}^{0}_{1}T\,{}^{1}_{2}T\,{}^{2}_{3}T \ldots {}^{N-1}_{N}T \quad (1) $$

The link-to-link transformation matrices are calculated using the DH parameters provided in Table I. As a result of these calculations,

the transformation matrix from the base to the end-effector is determined. The individual link-to-link transformation matrices for each joint are given below.

$$ {}^{0}_{1}T = \begin{bmatrix} c_1 & -s_1 & 0 & 0 \\ s_1 & c_1 & 0 & 0 \\ 0 & 0 & 1 & 0 \\ 0 & 0 & 0 & 1 \end{bmatrix} \quad (2) $$

$$ {}^{1}_{2}T = \begin{bmatrix} c_2 & -s_2 & 0 & 0 \\ 0 & 0 & 1 & 0 \\ -s_2 & -c_2 & 1 & 0 \\ 0 & 0 & 0 & 1 \end{bmatrix} \quad (3) $$

$$ {}^{2}_{3}T = \begin{bmatrix} c_3 & -s_3 & 0 & a_2 \\ s_3 & c_3 & 0 & 0 \\ 0 & 0 & 1 & d_3 \\ 0 & 0 & 0 & 1 \end{bmatrix} \quad (4) $$

$$ {}^{3}_{4}T = \begin{bmatrix} c_4 & -s_4 & 0 & 0 \\ 0 & 0 & -1 & -d_4 \\ s_4 & c_4 & 0 & 0 \\ 0 & 0 & 0 & 1 \end{bmatrix} \quad (5) $$

$$ {}^{4}_{5}T = \begin{bmatrix} c_5 & -s_5 & 0 & 0 \\ 0 & 0 & 1 & 0 \\ -s_5 & -c_5 & 0 & 0 \\ 0 & 0 & 0 & 1 \end{bmatrix} \quad (6) $$

$$ {}^{5}_{6}T = \begin{bmatrix} c_6 & -s_6 & 0 & 0 \\ 0 & 0 & -1 & -d_6 \\ s_6 & c_6 & 0 & 0 \\ 0 & 0 & 0 & 1 \end{bmatrix} \quad (7) $$

Where $s_i = \sin\theta_i$ and $c_i = \cos\theta_i$. Equation 8 shows the homogeneous transformation matrix from the base to end-effector. By applying this equation, the rotation and position components can be determined through matrix multiplication using the angles θ_1, θ_2, θ_3, θ_4, θ_5, and θ_6.

$$ {}^{0}_{6}T = {}^{0}_{1}T\,{}^{1}_{2}T\,{}^{2}_{3}T\,{}^{3}_{4}T\,{}^{4}_{5}T\,{}^{5}_{6}T \quad (8) $$

The upper-left 3 × 3 part of the transformation matrix in Equation 8 gives the rotation matrix of the robot arm, while the upper-right 3×1 part provides the position vector of the end-effector. The transformation matrix ${}^{0}_{6}T$ is given in Equation 9. By using the upper-left 3×3 part of the transformation matrix, the roll (α), pitch (β), and yaw (γ) angles can be calculated, and the upper-right 3×1 part gives the X, Y, and Z position of the end-effector.

$$ {}^{0}_{6}T = \begin{bmatrix} r_{11} & r_{12} & r_{13} & p_x \\ r_{21} & r_{22} & r_{23} & p_y \\ r_{31} & r_{32} & r_{33} & p_z \\ 0 & 0 & 0 & 1 \end{bmatrix} \quad (9) $$

Rotation to Euler equations to find the roll, pitch, and yaw angles are given in Equations 10, 11 and 12.

$$ \alpha = \arctan 2\,(r_{32},\ r_{33}) \quad (10) $$

$$ \beta = -\arcsin(r_{31}) \quad (11) $$

$$ \gamma = \arctan 2\,(r_{21},\ r_{11}) \quad (12) $$

Inverse Kinematics Model

Inverse kinematics is a fundamental concept in robotics that allows for the determination of joint variables necessary for a robotic manipulator to reach a specified end-effector position and orientation in three-dimensional space. By providing the desired spatial coordinates and orientation of the end-effector, inverse kinematic analysis systematically computes the required joint angles or displacements, enabling the robot to accurately perform complex tasks such as pick-and-place operations, path following, and precise manipulation within its workspace. This approach forms the basis for trajectory planning and advanced control strategies in robotic systems.

The algebraic solution technique, which is a type of closed-form solution method, applied for the Staubli robot manipulator model. In solving the inverse kinematics equations, both the transformation matrix from the base to the end-effector and the individual link transformation matrices are utilized. This approach enables the direct calculation of the joint variables required for the end-effector to achieve a desired pose.

In order to find the angles of the first three joints, the joint six was ignored to provide the necessary equations since it has no effect on the position vector. For the last three joints, the angles were calculated using the transformation matrices of the whole system. The joint angles θ_1 and θ_3 are calculated using the equation given below in Equation 13. θ_1 is calculated by equating the (2,4) elements on both sides of Equation 13. θ_3 is calculated by equating the (1,4) elements and (3,4) elements on both sides of Equation 13.

$$ \left[{}^{0}_{1}T^{-1}\,{}^{0}_{5}T\right] = {}^{1}_{2}T\,{}^{2}_{3}T\,{}^{3}_{4}T\,{}^{4}_{5}T \quad (13) $$

For the joint angle θ_2, the sum $\theta_2+\theta_3$ is obtained by equating the (1,4) and (2,4) elements of both sides in Equation 14. Since θ_3 is already known, θ_2 is found by subtracting θ_3 from $\theta_2+\theta_3$.

$$[{}^0_3T^{-1}\,{}^0_5T] = {}^3_4T\,{}^4_5T \quad (14)$$

For the joint angle θ_4, its value is determined by equating the (1,3) and (3,3) elements from both sides of Equation 15.

$$[{}^0_3T^{-1}\,{}^0_6T] = {}^3_4T\,{}^4_5T\,{}^5_6T \quad (15)$$

The angle θ_5 is calculated by equating the (1,3) and (3,3) elements of Equation 16.

$$[{}^0_4T^{-1}\,{}^0_6T] = {}^4_5T\,{}^5_6T \quad (16)$$

The angle θ_6 is calculated by equating the (3,1) and (1,1) elements of Equation 17.

$$[{}^0_5T^{-1}\,{}^0_6T] = {}^5_6T \quad (17)$$

DYNAMIC MODEL OF STAUBLI ROBOT ARM

Dynamic modeling is a critical aspect of robotic system analysis as it provides a mathematical framework for describing the relationship between joint torques and the resulting motion of the manipulator. Unlike kinematic analysis, which only considers geometric relationships, dynamic modeling includes inertial, Coriolis and centrifugal forces, and the effects of gravity. This comprehensive approach enables accurate prediction and control of a robot's motion, especially in tasks that require high speed or precise force application. In this study, Lagrange based dynamic analysis method is used. Kinetic energies and potential energies were calculated for each link.

The kinetic energy of the i_{th} link is given in Equation 18.

$$k_i = \frac{1}{2} m_i v_{C_i}^T v_i + \frac{1}{2} \boldsymbol{\omega_i^T I_{C_i} \omega_i} \quad (18)$$

The initial term quantifies the translational kinetic energy of the link's center of mass, whereas the subsequent term characterizes the rotational kinetic energy about that center.

Equation 19 shows that the total kinetic energy is summed over all kinetic energies of the links.

$$k = \sum_{i=1}^{n} k_i \quad (19)$$

Equation 20 expresses the total kinetic energy of the robot manipulator in joint space. Here, $\dot{\theta}$ is the joint velocity vector, and $M(\theta)$ represents the n×n inertia matrix, which depends on the joint positions θ.

$$k(\theta, \dot{\theta}) = \frac{1}{2} \dot{\theta}^T M(\theta) \dot{\theta} \quad (20)$$

The potential energy of the i_{th} link is given in Equation 21.

$$u_i = -m_i^0 g^T {}^0P_{C_i} + u_{ref_i} \quad (21)$$

where g is the gravity vector, P_{Ci} is the base frame position vector of the i_{th} link's center of mass. As shown in Equation 22, the total potential energy is obtained by summing the potential energy contributions from each individual link.

$$u = \sum_{i=1}^{n} u_i \quad (22)$$

The Lagrangian of the manipulator is given in Equation 23.

$$\mathcal{L}(\theta, \dot{\theta}) = k(\theta, \dot{\theta}) - u(\theta) \quad (23)$$

Equation 24 represents the fundamental dynamic equation of the robot manipulator, relating joint torques to the kinetic and potential energy of the system through the Lagrange formulation

$$\frac{d}{dt}\left(\frac{\partial k}{\partial \dot{\theta}}\right) - \frac{\partial k}{\partial \boldsymbol{\theta}} + \frac{\partial u}{\partial \boldsymbol{\theta}} = \boldsymbol{\tau} \quad (24)$$

The manipulator's dynamic equations are formulated as a function of the joint angles and their derivatives with respect to time, that is, in joint space, and can be represented in the general form shown in Equation 25

$$\tau = M(\theta)\ddot{\theta} + C(\theta,\dot{\theta})\dot{\theta} + G(\theta) \quad (25)$$

where C $(\theta, \dot{\theta})$ is a n×n Centripetal-Coriolis matrix and G(θ) is a n×1 gravitational vector.

In robotic dynamic modeling, the equations of motion can be linearly parameterized in terms of a regression matrix and a vector of dynamic parameters. This allows the dynamic model to be expressed in the form τ = W $(\theta, \dot{\theta}, \ddot{\theta})$ φ, where W is the regression matrix and φ is the vector of constant dynamic parameters such as masses, inertias, and link lengths. Furthermore, the matrix $\dot{M}(\theta) - 2C(\theta, \dot{\theta})$ is skew-symmetric, which is a key property used in Lyapunov-based stability analysis to show that certain energy terms cancel out, ensuring the boundedness of the system and convergence of the tracking errors.

ADAPTIVE CONTROLLER AND STABILITY ANALYSIS

This chapter presents the design of an adaptive control algorithm for the Staubli robot manipulator. Adaptive control methods are used to deal with uncertainties in system dynamics such as changes in payload, unmodeled dynamics and parameter changes. The proposed adaptive controller updates its parameters online in response to real-time errors between the desired and actual trajectories, ensuring robust performance even in the presence of significant model uncertainties. The stability of the robot's closed-loop system is rigorously established through a Lyapunov analysis, from which sufficient conditions are derived to ensure asymptotic convergence of the tracking error and uniform boundedness of all internal error terms. The block diagram of adaptive control is represented in Fig. 3.

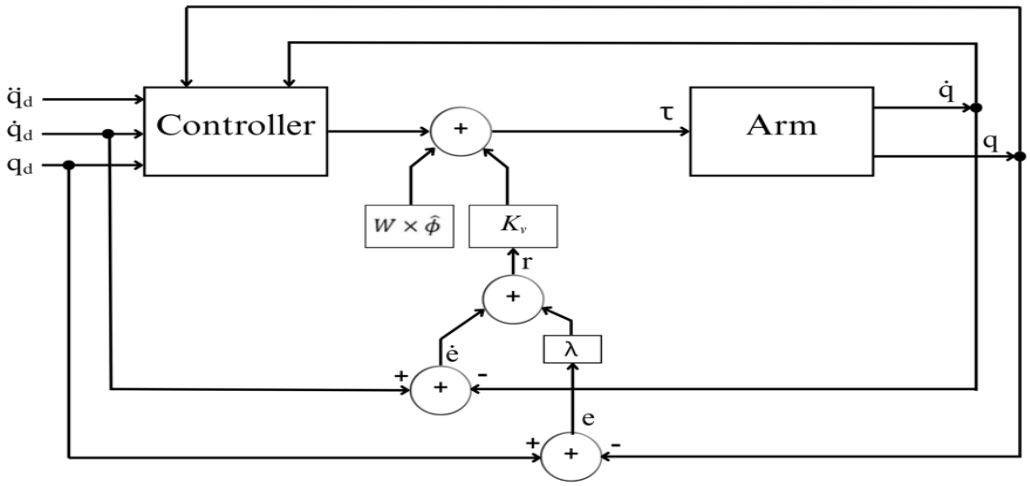

Fig. 3: Block diagram of adaptive control.

The position error term e represents the deviation from the desired position trajectory, while the velocity error term $\dot{e}$ denotes the deviation from the desired velocity trajectory, as defined in Equations 26 and 27. The auxiliary error-like term is also defined in Equation 28

$$e = \theta_d - \theta_a \quad (26)$$

$$\dot{e} = \dot{\theta}_d - \dot{\theta}_a \quad (27)$$

$$r = \dot{e} + \lambda e \quad (28)$$

where $\lambda \in R^{n\times n}$ positive definite control gain matrix.

In the presence of parametric uncertainties within the dynamic model, an adaptive controller is used to compensate for these uncertain or time-varying parameters and

ensure that the desired control objectives are achieved.
The adaptive controller τ(t) is designed as

$$\tau = K_v r + W\hat{\phi} \quad (29)$$

where $K_v \in R^{n\times n}$ is a constant diagonal and positive definite control gain matrix, $r(t) \in R^n$ is an auxiliary error-like term, W is 6×78 regression matrix, and $\hat{\varphi} \in R^p$ is the estimation of the unknown parameter vector φ. The estimation of $\hat{\varphi}$ is updated based on the adaptive law given in Equation 30.

$$\dot{\hat{\phi}} = \Gamma W^T r \quad (30)$$

where $\Gamma \in R^{p\times p}$ is a constant diagonal and positive definite adaptation gain matrix. For stability analysis, the Lyapunov function V(t) selected by considering the inertia characteristics of the robot and the defined error terms (both for controller and adaptive law) is given as

$$V = \frac{1}{2} r^T M r + \frac{1}{2} \tilde{\phi}^T \Gamma^{-1} \tilde{\phi} \quad (31)$$

where $\tilde{\varphi} \in R^p$ is the parameter estimated error and is defined as

$$\tilde{\phi} = \phi - \hat{\phi} \quad (32)$$

The time derivative $\dot{V}(t)$ of the Lyapunov function V(t) is taken as

$$\dot{V} = r^T M \dot{r} + \frac{1}{2} r^T \dot{M} r + \tilde{\phi}^T \Gamma^{-1} \dot{\tilde{\phi}} \quad (33)$$

Substituting the above robot dynamics and error equations into equation 33, using the adaptation rule 30, the parameter error term 32, and the robot dynamics and skew-symmetric properties, $\dot{V}$ can be rewritten in the following form after mathematical manipulations

$$\dot{V} = -r^T K_v r \quad (34)$$

Since K_v is positive definite, inequality $\dot{V} \leq 0$ shows that $\dot{V}$ is negative semi-definite. The Lyapunov function V is positive definite and lower bounded, while $\dot{V}$ is negative semi-definite. In this context, Barbalat's Lemma is applied as

$$\lim_{t\to\infty} \dot{V} = 0 \quad (35)$$

$$\lim_{t\to\infty} \lambda_{min}\{K_v\}||r||^2 = 0 \quad \text{or} \quad \lim_{t\to\infty} r = 0 \quad (36)$$

Finally, from equation 28, it can be said that both the position error e and the velocity error $\dot{e}$ converge to zero.

$$\lim_{t\to\infty} e = 0 \quad \text{and} \quad \lim_{t\to\infty} \dot{e} = 0 \quad (37)$$

The stability analysis confirms that the position error e and the velocity error $\dot{e}$ converge asymptotically to zero, while the parameter estimation error remains bounded. Consequently, the proposed adaptive controller ensures asymptotic tracking of the desired trajectory.

SIMULATION STUDIES AND RESULTS

In this section, simulation studies are performed to evaluate the performance of the developed adaptive control scheme in the presence of dynamic uncertainties. Fig. 4 shows the adaptive controller in MATLAB Simulink.

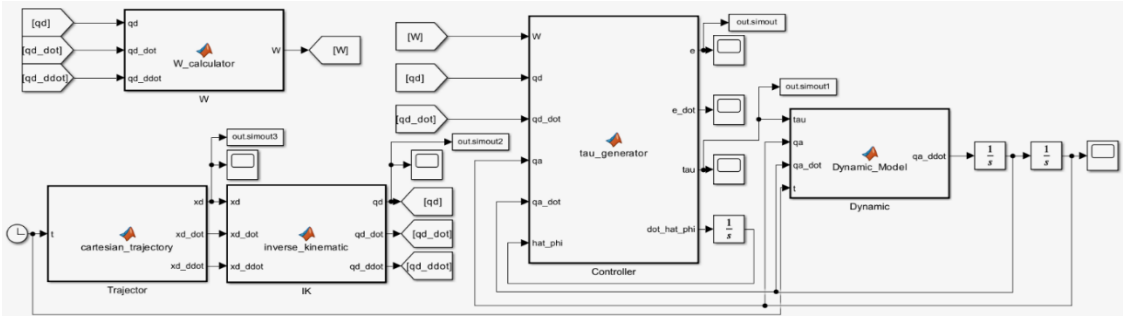

Fig. 4: Adaptive control in Simulink.

The controller gains mentioned in the Adaptive Controller Section and included in Equations 28, 29 and 30 are given below.

$K_v = diag[500,500,500,500,500,500]$	(38)
$\lambda = diag[600,600,600,600,600,600]$	(39)
$\Gamma = 5 \times I(78)$	(40)

In the simulation study, three different test cases are designed by varying the payload mass connected to the end-effector of the robot manipulator. These variations are aimed at evaluating the controller's ability to compensate for changing dynamic parameters. The results are analyzed in terms of joint tracking accuracy and control effort. The results obtained confirm that the adaptive controller successfully maintains system stability and provides accurate trajectory tracking under different load conditions.

Case 1

In Case 1, simulation is designed without any weights on the end-effector. Fig. 5 shows the result of this case.

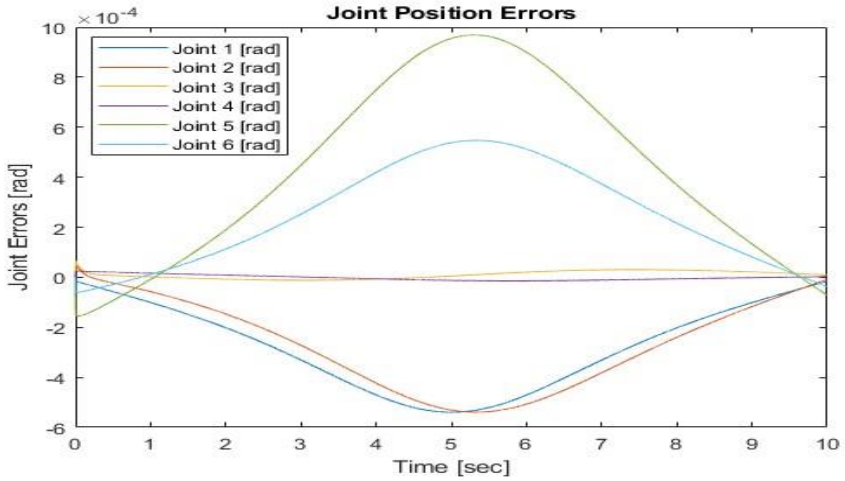

Fig. 5: Joint position errors for case 1.

In this case, as can be seen in Figure 5, all joints of the robot arm perform the desired joint positions perfectly for 10 seconds.

Case 2

In Case 2, the robot manipulator with its end-effector is simulated picks up a load of 1 kilogram in the third second and places it down in the seventh second. Fig. 6 shows the result of this case.

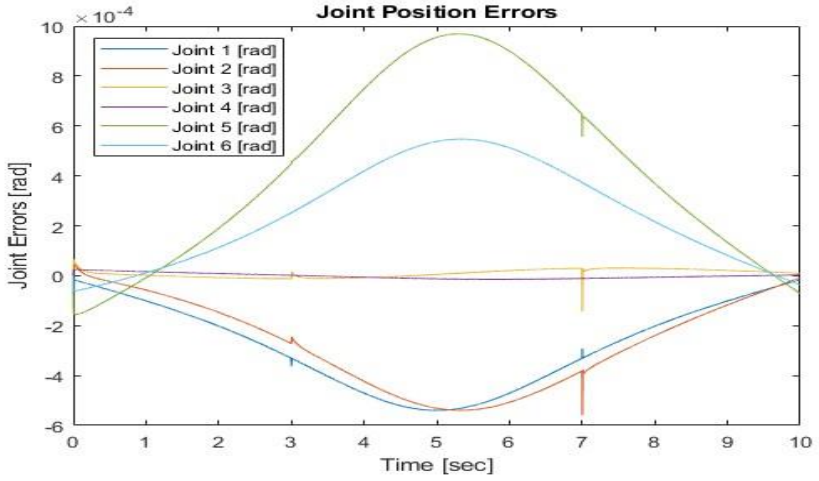

Fig. 6: Joint position errors for case 2.

In this case result shown in Figure 6, the instantaneous change in the load carried by the robot arm affected all joints, although very slightly, but it still performed the desired joint movements almost perfectly for 10 seconds.

Case 3

In Case 3, 1 kilogram of weight is linearly loaded into a bucket in the end-effector of the robot arm from the beginning to the fourth second, this weight is maintained between the fourth and sixth seconds, and the unloading of the bucket from the sixth second to the end is simulated and Fig. 7 shows the result of this case.

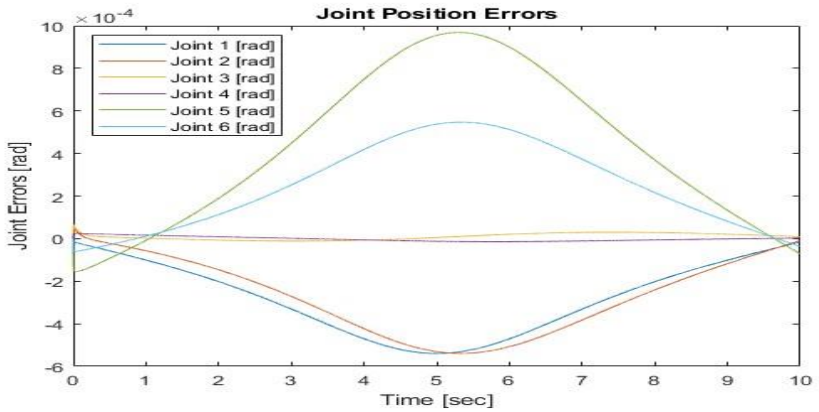

Fig. 7: Joint position errors for case 3.

In this case shown in Figure 7, the controller has adapted very well to changes in the loads carried by the robot arm over time and performs the desired joint movements with almost zero error for 10 seconds.

DISCUSSION

In the first case, the robot arm was able to follow the desired joint trajectories with remarkable precision for the entire 10-second duration, showing almost no noticeable position error. This shows that the adaptive controller performs effectively under nominal conditions without additional payload disturbances. In the second case, a sudden 1 kg payload was applied to the end-effector. Although this instantaneous change slightly affected all joints, the controller quickly adapted and the robot continued to track the desired trajectories with only minimal deviation, maintaining stable and accurate motion. The third case introduced a linearly varying payload over time, which posed a more challenging scenario for the controller. Even under these gradual changes, the adaptive controller responded smoothly, continuously adjusting to the shifting dynamics and keeping the tracking error very close to zero across all joints. Together, these results highlight the robustness and adaptability of the proposed control approach, showing that it can maintain precise and reliable performance even under sudden or continuously varying payload conditions.

CONCLUSION

This study has presented the design, analysis, and validation of an adaptive tracking control strategy for a 6-DOF Staubli TX2-60L industrial robot manipulator operating under dynamic uncertainties induced by varying payloads. Beginning with the derivation of the complete kinematic and dynamic models through Denavit–Hartenberg parameters and Lagrangian formulation, a solid theoretical foundation was established for developing a control framework capable of handling parameter variations and unmodeled dynamics. Building on this foundation, an adaptive controller was designed to update its parameters online, allowing the system to respond effectively to unpredictable disturbances and payload changes that are

commonly encountered in industrial environments.

The stability of the proposed approach was rigorously demonstrated through Lyapunov-based analysis, showing that both position and velocity tracking errors converge asymptotically while the parameter estimation errors remain bounded. This theoretical guarantee was further supported by comprehensive simulation studies, which evaluated the controller under three distinct scenarios: nominal operation without payload, abrupt step changes in load, and continuous linear variations in payload. In all cases, the adaptive controller proved capable of maintaining precise trajectory tracking and stable system behavior, even under sudden or gradually changing conditions. These results highlight the controller's robustness, adaptability, and suitability for real-world industrial applications where high reliability and precision are non-negotiable.

Beyond the technical achievements, the findings also point to broader implications for robotics in modern manufacturing. Industrial manipulators are increasingly required to operate in dynamic and unpredictable environments, often in collaboration with human workers or in tasks where payloads and external conditions can change rapidly. By demonstrating a control approach that adapts in real time to such uncertainties, this work contributes toward bridging the gap between theoretical control methods and the practical demands of Industry 4.0. The adaptability and robustness achieved here not only enhance operational accuracy but also improve safety and reduce downtime, thereby supporting the growing need for intelligent, resilient, and human-centered automation systems.

In conclusion, the proposed adaptive control strategy has demonstrated strong potential for enabling industrial robots to operate reliably and efficiently in the face of dynamic uncertainties. By uniting solid theoretical analysis with practical validation, this work lays a foundation for future advancements in adaptive and intelligent robotic systems, contributing to the vision of resilient, flexible, and human-aware automation in next-generation manufacturing environments.

Declaration by Authors

Acknowledgement: We would like to thank the Scientific and Technological Research Council of Turkiye (TUBITAK) (Project number: 5240102) within the scope of TEYDEB-1505 University-Industry Cooperation Project.

Source of Funding: None.

Conflict of Interest: The authors declare no conflict of interest.

REFERENCES

1. G.-Z. Yang, J. Bellingham, P. E. Dupont, P. Fischer, L. Floridi, R. Full, N. Jacob- stein, V. Kumar, M. McNutt, R. Merrifield, et al., "The grand challenges of science robotics," Science robotics, vol. 3, no. 14, p. eaar7650, 2018.
2. J. Arents and M. Greitans, "Smart industrial robot control trends, challenges and opportunities within manufacturing," Applied Sciences, vol. 12, no. 2, p. 937, 2022.
3. J. Tian, Y. Zhou, L. Yin, S. A. Alqahtani, M. Tang, S. Lu, R. Wang, and W. Zheng, "Control structures and algorithms for force feedback bilateral teleop- eration systems: A comprehensive review.," Computer Modeling in Engineering & Sciences (CMES), vol. 142, no. 2, 2025.
4. A. C. Emmanuel and H. Inyiama, "A survey of controller design methods for a robot manipulator in harsh environments," European Journal of Engineering and Technology Vol, vol. 3, no. 3, 2015.
5. V. Tinoco, M. F. Silva, F. N. Santos, R. Morais, S. A. Magalh˜aes, and P. M. Oliveira, "A review of advanced controller methodologies for robotic manipu- lators," International Journal of Dynamics and Control, vol. 13, no. 1, p. 36, 2025.
6. Xu, K., Wang, Z. The design of a neural network-based adaptive control method for robotic arm trajectory tracking. Neural Comput & Applic 35, 8785–8795 (2023).
7. M. Pascher, K. Kronhardt, F. F. Goldau, U. Frese and J. Gerken, "In Time and Space: Towards Usable Adaptive Control for Assistive Robotic Arms," 2023 32nd IEEE

International Conference on Robot and Human Interactive Communication (RO-MAN), Busan, Korea, Republic of, 2023, pp. 2300-2307, doi: 10.1109/RO-MAN57019.2023.10309381.
8. Shang, D., Li, X., Yin, M., & Li, F. (2022). Dynamic modeling and fuzzy adaptive control strategy for space flexible robotic arm considering joint flexibility based on improved sliding mode controller. Advances in Space Research, 70(11), 3520-3539.
9. Tuan, H. M., Sanfilippo, F., & Hao, N. V. (2022). A Novel Adaptive Sliding Mode Controller for a 2-DOF Elastic Robotic Arm. Robotics, 11(2), 47. https://doi.org/10.3390/robotics11020047
10. M. S. Nazeer, C. Laschi and E. Falotico, "RL-Based Adaptive Controller for High Precision Reaching in a Soft Robot Arm," in IEEE Transactions on Robotics, vol. 40, pp. 2498-2512, 2024, doi: 10.1109/TRO.2024.3381558.
11. Liu, A., Zhao, H., Song, T. et al. Adaptive control of manipulator based on neural network. Neural Comput & Applic 33, 4077–4085 (2021). https://doi.org/10.1007/s00521-020-05515-0
12. Deylami A, Izadbakhsh A. FAT-based robust adaptive control of cooperative multiple manipulators without velocity measurement. Robotica. 2022;40(6):1732-1762. doi:10.1017/S0263574721001338
13. Chaure, R. S. (2021). Adaptive control of a DDMR with a Robotic Arm (Doctoral dissertation, Virginia Tech).
14. Seghiri, T., Ladaci, S., & Haddad, S. (2023). Fractional order adaptive MRAC controller design for high-accuracy position control of an industrial robot arm. International Journal of Advanced Mechatronic Systems, 10(1), 8-20.
15. Hasanpour, H., Alibeiki, E., & Ghadami, S. M. (2022). Flexible Robot Arm Control Using Adaptive Control Structure. Journal of Applied Dynamic System and Control, 5(1), 5-10.
16. Zahaf, A., Bououden, S., Chadli, M., & Chemachema, M. (2022). Robust fault tolerant optimal predictive control of hybrid actuators with time-varying delay for industrial robot arm. Asian Journal of Control, 24(1), 1-15.
17. H. -T. Zhang, H. Xu, B. Xu, Y. Wu, J. Huang and Q. -L. Han, "Adaptive Learning-Based Distributed Control of Cooperative Robot Arm Manipulation for Unknown Objects," in IEEE Transactions on Systems, Man, and Cybernetics: Systems, vol. 53, no. 2, pp. 1298-1307, Feb. 2023, doi: 10.1109/TSMC.2022.3197664.
18. Yin, X., Pan, L., & Cai, S. (2021). Robust adaptive fuzzy sliding mode trajectory tracking control for serial robotic manipulators. Robotics and Computer-Integrated Manufacturing, 72, 101884.
19. Cheng, X., Zhou, J., Zhou, Z., Zhao, X., Gao, J., & Qiao, T. (2023). An improved RRT-Connect path planning algorithm of robotic arm for automatic sampling of exhaust emission detection in Industry 4.0. Journal of Industrial Information Integration, 33, 100436.
20. Xue, X., Huang, H., Zuo, L., & Wang, N. (2022). A compliant force control scheme for industrial robot interactive operation. Frontiers in neurorobotics, 16, 865187.

How to cite this article: Emir Sonmez, Kamil Cetin. Adaptive tracking control for dynamic model uncertainties of a 6-DOF industrial Staubli robot manipulator carrying variable payloads. *International Journal of Research and Review*. 2025; 12(9): 661-672. DOI: *https://doi.org/10.52403/ijrr.20250963*

******